Available online at www.sciencedirect.com
ScienceDirect
Journal of Nuclear Materials 375 (2008) 382–387
journal of nuclear materials
www.elsevier.com/locate/jnucmat

Root causes of intergranular attack in an operating nuclear steam generator tube

Do Haeng Hur [a,*], Deok Hyun Lee [a], Myung Sik Choi [a], Myung Ho Song [b], Jung Ho Han [a]

[a] Korea Atomic Energy Research Institute, 150 Deokjin-dong, Yuseong-gu, Daejeon 305-353, Republic of Korea
[b] Korea Institute of Nuclear Safety, 19, Guseong-dong, Yuseong-gu, Daejeon 305-338, Republic of Korea

Received 6 November 2007; accepted 23 January 2008

Abstract

This paper reports the secondary side intergranular attack of an Alloy 600 tube, which was located within sludge piles in the hot-leg side of an operating nuclear steam generator. Carbide distribution along the grain boundaries and chromium depletion were analyzed using optical microscopy and transmission electron microscopy. Local crevice chemistry in contact with the defect was also assessed from the hideout return test data and oxide film analysis results using energy dispersive spectroscopy. The main causes of this defect are discussed based on the microstructure, local chemistry and operation temperature.
© 2008 Elsevier B.V. All rights reserved.

1. Introduction

Because steam generator tubes are a pressure boundary between the primary coolant system and the secondary coolant system in pressurized water reactor (PWR) nuclear power plants, the integrity of steam generator tubes is essential for operational safety. Unfortunately, some steam generator tubes have been affected by corrosion and mechanical degradation such as stress corrosion cracking, intergranular attack (IGA), wear and fatigue [1]. Eddy current testing (ECT) is widely used to detect such defects occurring in these tubes and to monitor the growth of pre-existing flaws during an in-service inspection.

As the tubes are equipped in steam generators, it is impossible to directly evaluate the main causes, type and size of defects occurring in these tubes. Pulling of damaged tubes from steam generators and subsequent destructive examination are the only path to overcome these problems. Therefore, from pulled tube examinations, we can elucidate the main causes of a degradation and validate an ECT reliability of detection and sizing accuracy for defects. Furthermore, strategies to mitigate tube degradation can be effectively established. However, this method has several disadvantages such as radiation exposure, extended overhaul period, and limited number of pulled tubes. Nevertheless, the results of pulled tube examinations are extremely valuable.

In this work, destructive examinations of a defective tube removed from an operating PWR steam generator are described. This steam generator was constructed with high temperature mill-annealed Alloy 600 tubes with a 19.05 mm outer diameter (OD) and a 1.07 mm wall thickness. These tubes were explosively expanded over the full depth of the low alloy steel tube sheet. The secondary water for the steam generators have been chemically treated with an all-volatile treatment (AVT) from a plant startup. As corrosion defects on the outer diameter side of tubes in this steam generator were detected first by an ECT at the 5th end of fuel cycle (EOC) in 2004, a tube pull examination was conducted at the 6th EOC in 2006 to determine the root causes of the degradation and to validate the reliability of the ECT. In this work, results of the detailed destructive analysis such as the microstructure, fractography and local crevice chemistry are presented. Based on these results, main causes of this defect are discussed based on

* Corresponding author. Tel.: +82 42 868 8388; fax: +82 42 868 8304.
E-mail address: dhhur@kaeri.re.kr (D.H. Hur).

0022-3115/$ - see front matter © 2008 Elsevier B.V. All rights reserved.
doi:10.1016/j.jnucmat.2008.01.017

the microstructure, local chemistry and operation temperature. A detailed comparison of the ECT results and the destructive examination results are given elsewhere [2].

2. Experimental methods

A tube with an eddy current defect signal on the outer diameter side was selected for removal and destructive examination, which was located in the hot-leg side of a steam generator. The defect was estimated by an ECT to be present at a location of 3 mm above the top of the tube sheet (TTS). The selected tube was loosened by heat shrinking the section within the tube sheet and then pulled by a radial gripping from the tube inner surface. The location for the heat shrinking and gripping was below the defect position so that the defect was not deformed.

The pulled tube was transferred into a hot laboratory. In order to observe the as-received condition of the tube segment, photographs from the outer surface of the pulled tube were taken using a high-resolution digital camera after successive rotations of 22.5°.

As no defects were identified from the visual inspection, a region from TTS − 10 mm to TTS + 18 mm was sectioned into 39 segments by cutting it in the longitudinal and circumferential directions of the tube. The cross sections of the segments were mounted in resin, ground successively with silicon carbide (SiC) paper up to 2000 grit and polished with 0.05 μm alumina (Al_2O_3) powder. Then, the defect morphology was observed by optical microscopy. Chemical analysis for the oxide films was also made by energy dispersive spectroscopy (EDS) to elucidate the local chemistry condition in contact with the surface of the defected tube.

The duel step etch technique was used to examine the carbide distributions and the grain morphologies. That is, polished cross sections were etched first in phosphoric acid to delineate the carbides and then in 5% nital solution to reveal grain boundaries. Detailed microstructure analysis was also performed using transmission electron microscopy (TEM). Thin foils were prepared by jet thinning sample discs in 93% methanol + 7% perchloric solution at −50 °C and at a current range of 30–50 mA. All the specimens for microstructure observations were prepared from the sections at about TTS + 120 mm elevation of the pulled tube.

3. Results

3.1. Fractography

Fig. 1(a) shows a figure of the as-received OD condition of the pulled tube. The TTS line was defined well and the profile of the sludge accumulated around the tube was also clearly identified. The circle corresponds to the location of the defect signal in Fig. 1(b), which was detected by a plus point coil [3] mounted in a motorized eddy current probe at a frequency of 300 kHz. However, no defect was observed from the visual inspection.

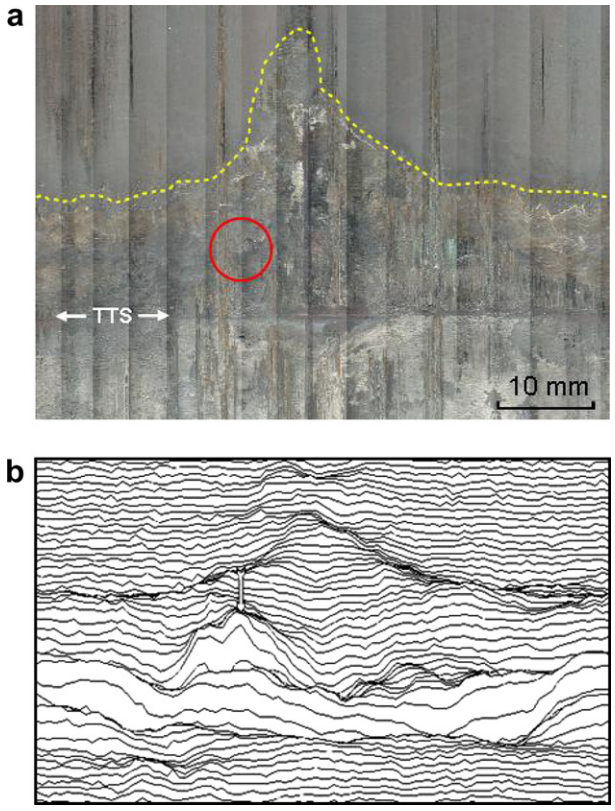

Fig. 1. (a) Outer surface of pulled tube and (b) ECT result.

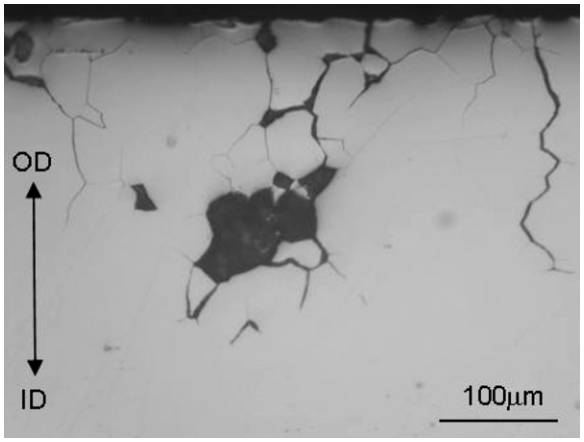

Fig. 2. Cross sectional view showing IGA.

Nevertheless, numerous defects were revealed by metallographic examinations. Fig. 2 shows a cross section at TTS + 8 mm, corresponding to the central location of the defect indication signal. Grain boundaries were attacked and several grains had dropped out. This type of defect was a typical IGA. Similar defects including minor intergranular stress corrosion cracks (IGSCC) were also observed in many other segments.

The final result is summarized in Fig. 3. Defects were found in two regions. That is, this type of IGA extended to all over the each region. Defect region A correlated well with the EC defect signal location. In this region, the max-

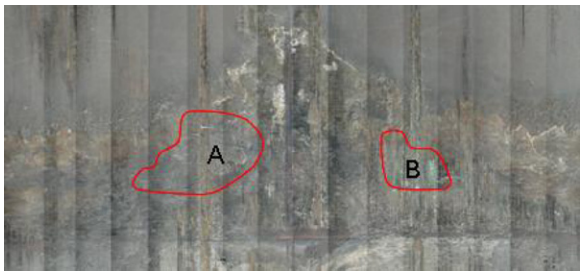

Fig. 3. Defect regions on the outer surface.

imum depth of the penetration was 28% of the tube wall thickness. Region B indicated no defect signal, but showed IGA/IGSCC with a maximum depth of 16%. This means that it was below a detectable size of the ECT. It should also be noted that these defects were located inside sludge piles and above the expansion transition region.

3.2. Microstructure

Dual step etch microstructure of a longitudinal section near the defect region is shown in Fig. 4. A discrete decoration of carbides was observed along the grain boundaries with very sparse intragranular carbides. Average grain size determined by a linear intercept method was 68 μm, which was within the specification of a mill-annealed tube.

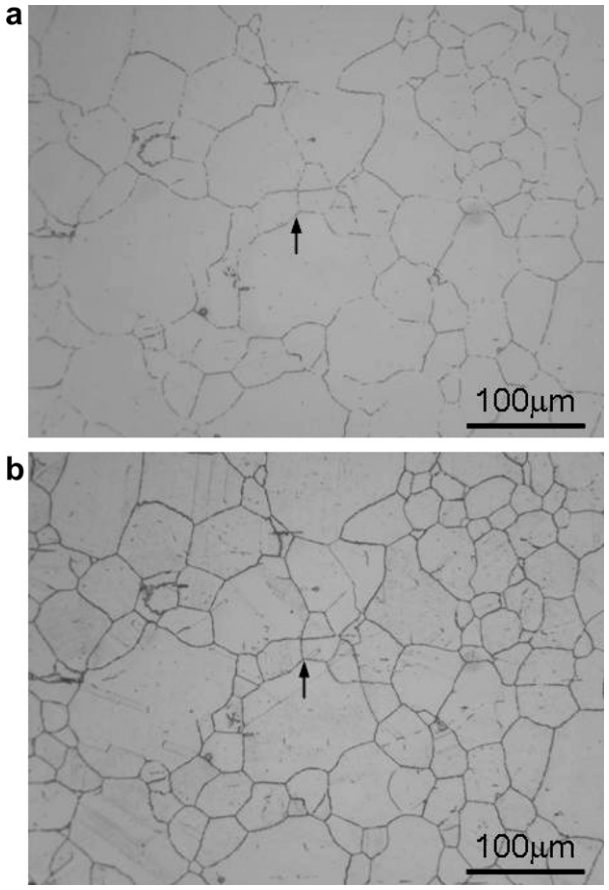

Fig. 4. Dual step etch micrographs. (a) Phosphoric etch and (b) nital etch.

All the grain boundary carbides analyzed by TEM were identified to be chromium rich M_7C_3. Chemical analysis showed these carbides to be 86–92 wt% chromium. Detailed examinations [4–6] have established that the form of the carbide in Alloy 600 is predominantly M_7C_3 rather than $M_{23}C_6$. However, its form and shape depend on the aging temperature and time [4,7].

As IGA has been directly correlated with chromium depletion at grain boundaries [8,9], the chromium content at the grain boundaries was measured by TEM-EDS. Fig. 5 shows the morphology of M_7C_3 carbides and the profile of chromium concentration across a grain boundary between two carbides. Chromium content at the grain boundaries was found to decrease to a range of 11.8–13.8 wt%. These values were a maximum of 7 wt% lower than the chromium content of the matrix. This means that the tube was slightly sensitized.

3.3. Local crevice chemistry assessment

Local crevice environments were deduced from the hide-out return test results implemented for this steam generator

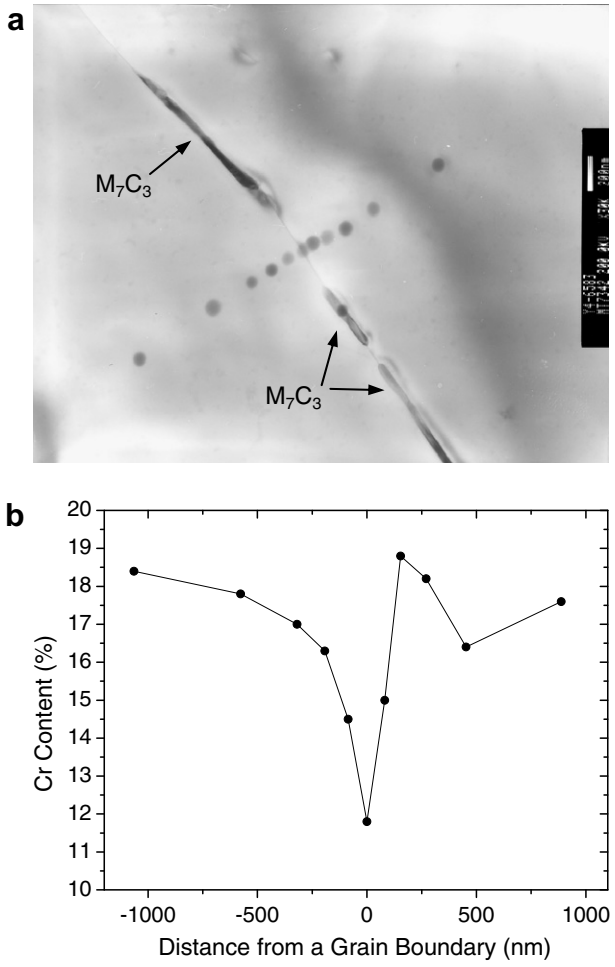

Fig. 5. (a) Carbide morphology and (b) chromium content profile across a grain boundary.

Table 1
MRI calculated by the hideout return data

EOC	1	2	3	4	5	6
MRI	2.52	8.53	0.67	Not performed	5.66	4.70

during the power reduction at the end of each fuel cycle (EOC). The result was analyzed by using a molar ratio index (MRI) defined as follows [10]:

$$\mathrm{MRI} = \frac{[\mathrm{Na}] + [\mathrm{K}]}{[\mathrm{Cl}] + \mathrm{excess}[\mathrm{SO_4}]} \quad (1)$$

where the molar concentration of each impurity species to be input into the MRI equation is obtained by performing a hideout return test. Here, a neutral pH is defined at a MRI of 1.0 and the pH becomes alkaline at MRI's larger than 1.0. The MRI's calculated by Eq. (1) are given in Table 1. These values except at EOC 3 indicate that the crevice chemistry was alkaline. The low MRI at EOC 3 can be attributed to an increase of sulfate ion, which may leak from the cation resin regeneration equipment.

The chemical composition analysis of the oxide film on the defect surface can provide more reliable information of a local crevice pH, because the solubility of chromium and nickel is dependant on the pH. Fig. 6 shows the X-ray mapping result for the oxide film formed on the cross sectional surface of the IGA region. This film was the as-grown oxide with a thickness of about 3 μm, not the deposits. It was therefore considered that a more reliable interpretation of the local crevice environments could be achieved. This oxide film was found to be depleted in chromium and enriched in nickel. The same trend was also observed at different analysis locations, although there was a small change in the degree of chromium depletion. According to the Pourbaix diagrams of chromium, nickel and iron [11], nickel has the broadest range of solid stability at high pH's with a stable nickel oxide, whereas chromium has the least solid stability. Similarly, it was reported that as the pH increased, the chromium content decreased uniformly and the nickel enriched uniformly in the surface film formed on Alloy 600 [12,13]. Hence, the oxide film composition analysis in Fig. 6 clearly indicates that the local chemistry in contact with the IGA was alkaline.

In addition, other impurities such as potassium, calcium and sulfur were detected on the outer surface deposits of the defect area by EDS, as shown in Fig. 7. It should be noted that sulfur compounds have been known to induce a film breakdown and thus accelerate IGA/IGSCC of Alloy 600 [14,15].

4. Discussion

IGA was found in two separate regions of the free span of the pulled tube, which was located within sludge piles in

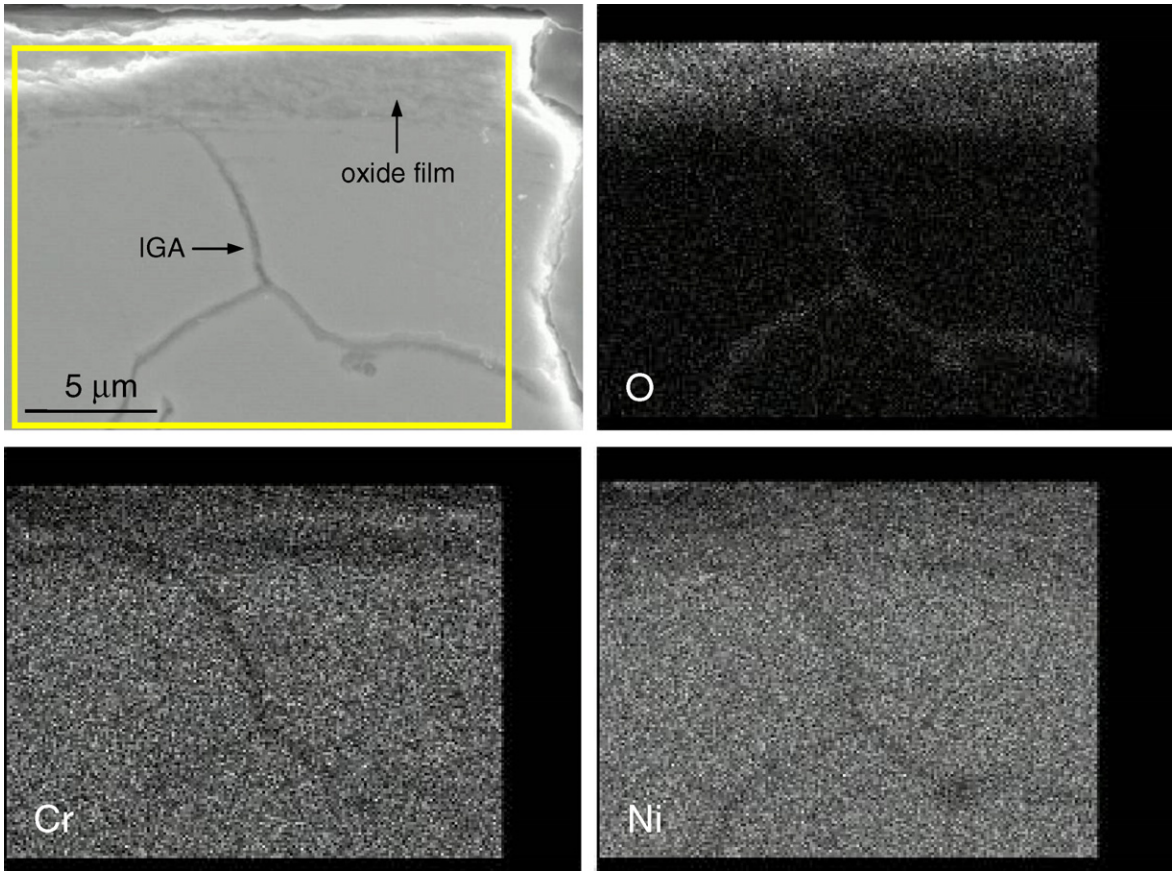

Fig. 6. Cross section near IGA and X-ray mapping.

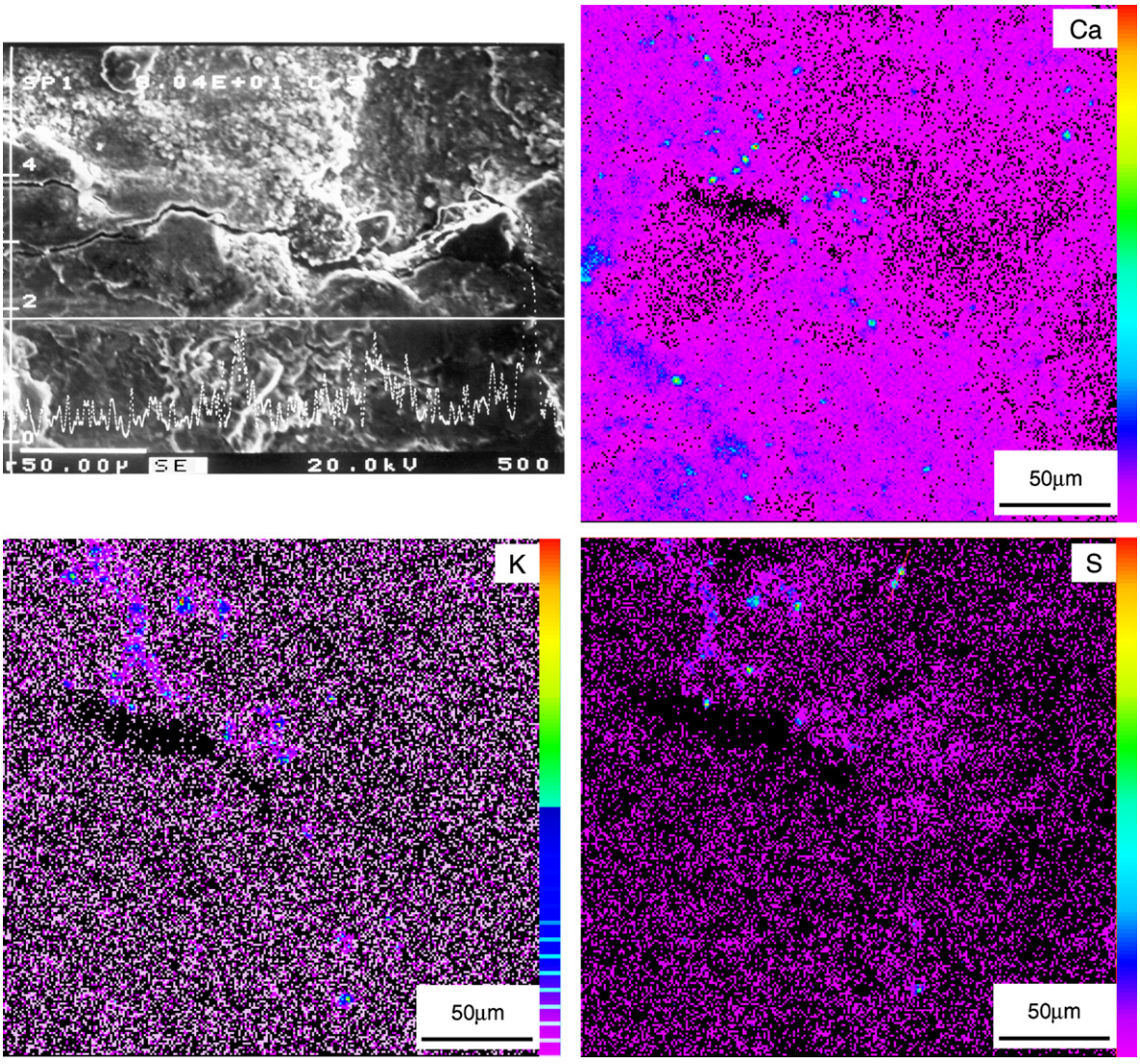

Fig. 7. X-ray mapping on the outer surface oxide of the defect area.

the hot-leg side of the steam generator. The maximum depth of the penetration was 28% of the tube wall thickness.

The microstructural observations showed that the grain boundaries were decorated with chromium carbides. However the chromium contents at the grain boundaries suggested that the tube was slightly sensitized. It has been reported that IGA of Alloy 600 was closely related with a grain boundary chromium depletion [8,9] and its rates rapidly increased as the pH became both acidic and alkaline [10].

The MRI data from the hideout return test results indicated that the crevice near the tube sheet had an alkaline environment. Moreover, chemical analysis for the oxide films clearly confirmed that the local pH in contact with the IGA was alkaline. Sulfur compounds were also detected on the deposits near the defects and could have contributed to the IGA. These chemicals appeared to be concentrated in the sludge piles and the tube sheet crevice by an evaporation of water at the tube surface, resulting in an alkaline environment. Hideout of sodium and potassium can be easier than that of anions, since acids such as H_2SO_4 and HCl are more volatile than alkaline compounds such as NaOH and KOH [16]. Hence, the local pH under the sludge piles on the TTS in the hot-leg side tends to become alkaline.

The IGA growth was thermally activated with an activation energy of about 31 kcal/mole in a caustic solution [17]. Therefore, the IGA has occurred preferentially in higher temperature locations such as the hot-leg tube sheet crevices and sludge piles. This is because the operating temperature is higher than that in the cold leg side and also the sludge plies increase the superheat by hindering a heat transport, which in turn result in high concentrations of impurities. In the case of this defective tube, the operating temperature of the primary side was 325 °C, which is very high relative to other types of steam generators. Therefore the high operating temperature of the primary side of this defective tube was considered to be another main cause of IGA.

5. Summary

IGA with a maximum penetration depth of 28% was found in two separate regions of the pulled tube within the sludge piles in the hot-leg side of the steam generator. Its main causes were analyzed as follows:

- The sludge piles around the defective tube formed crevices to concentrate corrosive impurities.
- The grain boundaries of the defective tube were slightly sensitized although they were decorated with chromium carbides.
- The MRI data and relative depletion of chromium in the oxide film suggested that the local environment of the IGA was alkaline.
- The high operating temperature of the primary side was considered to be another cause of IGA.
- Sulfur detected in the deposits could have contributed to the IGA.

Acknowledgement

This work was carried out as a part of the Nuclear R&D Program supported by the Ministry of Science and Technology in Korea.

References

[1] J. Benson, Steam generator progress report, EPRI TE-106365-R14, Palo Alto, CA; Electric Power Research Institute, 1998.
[2] D.H. Hur, M.S. Choi, D.H. Lee, J.H. Han, Nucl. Eng. Des., submitted for publication.
[3] J. Siegel, Nucl. Eng. Int. 41 (1996) 18.
[4] E.L. Hall, C.L. Briant, Metall. Trans. A 16A (1985) 1225.
[5] G.S. Was, R.M. Kurger, Acta Metall. 33 (1985) 841.
[6] J.J. Kai, C.H. Tsai, T.A. Huang, M.N. Liu, Metall. Trans. A 20A (1989) 1077.
[7] G.S. Was, J.R. Martin, Metall. Trans. A 16A (1985) 349.
[8] G.S. Was, H.H. Tichner, R.M. Latanision, Metall. Trans. A 12A (1981) 1397.
[9] G.P. Airey, Corrosion 41 (1985) 2.
[10] Molar ratio control guidelines committee, PWR molar ratio control application guidelines, vol. 1, EPRI TR-104811-V1, Palo Alto, CA, Electric Power Research Institute, 1995.
[11] P.L. Daniel, S.L. Harper, Use of Pourbaix diagram to infer local pitting conditions, EPRI NP-4831, Palo Alto, CA, Electric Power Research Institute, 1986.
[12] J.B. Lumsden, P.J. Stocker, A.R. Mcllree, Insights on local chemistry from examination of tubes, in: Proceedings of Control of Corrosion on the Secondary Side of Steam Generators, p. 473, NACE, 1996.
[13] H. Takamatsu, K. Matsueda, K. Onimura, K. Arioka, S. Tokunga, K. Katsura, IGA/IGSCC propagation behaviors of Alloy 600, in: Proceedings of the 4th International Symposium on Environmental Degradation of Materials in Nuclear Power Systems-Water Reactors, 1989, Jekyll Island, USA, p. 7–29, 1990.
[14] R.C. Newman, R. Roberge, R. Bandy, Corrosion 39 (1983) 386.
[15] Z. Fang, R. Staehle, Corrosion 55 (1999) 355.
[16] J.A Gorman, J.N. Paine, K.D. Stavropoulos, M.J. Partridge, Tube supports and tube sheet corrosion-alkaline denting, in: Steam Generator Reference Book, vol. 2/3, TR-103824, p. 11-6, EPRI, 1994.
[17] O. Cayla, P. Combrade, P. Malagola, G. Slama, Corrosion/85, paper no. 90, 1985.